



## ABSTRACT

9 Environmental variables are routinely used in estimating when and where tornadoes are likely to  
10 occur, but more work is needed to understand how tornado and casualty counts of severe weather  
11 outbreak vary with the larger scale environmental factors. Here the authors demonstrate a method  
12 to quantify ‘outbreak’-level tornado and casualty counts with respect to variations in large-scale  
13 environmental factors. They do this by fitting negative binomial regression models to cluster-level  
14 environmental data to estimate the number of tornadoes and the number of casualties on days with  
15 at least ten tornadoes. Results show that a  $1000 \text{ J kg}^{-1}$  increase in CAPE corresponds to a 5%  
16 increase in the number of tornadoes and a 28% increase in the number of casualties, conditional  
17 on at least ten tornadoes, and holding the other variables constant. Further, results show that  
18 a  $10 \text{ m s}^{-1}$  increase in deep-layer bulk shear corresponds to a 13% increase in tornadoes and a  
19 98% increase in casualties, conditional on at least ten tornadoes, and holding the other variables  
20 constant. The casualty-count model quantifies the decline in the number of casualties per year and  
21 indicates that outbreaks have a larger impact in the Southeast than elsewhere after controlling for  
22 population and geographic area.

## 23 1. Introduction

24 Estimating tornado and casualty counts (hereafter referred to as characteristics) of severe weather  
25 outbreaks is an important and challenging problem. It is important because of the potential for  
26 loss of life and property damage. It is challenging because of the uncertainties associated with  
27 exactly how many and where the tornadoes will occur. But progress is being made. Guidance from  
28 dynamical models help forecasters outline areas of possible severe weather threats days in advance  
29 (Hitchens and Brooks 2014) while guidance from statistical models help forecasters quantify  
30 probabilities for given severe weather events (Thompson et al. 2017; Cohen et al. 2018; Elsner  
31 and Schroder 2019; Hill et al. 2020). For example, Cohen et al. (2018) use a regression model  
32 to specify the probability of tornado occurrence given certain environmental and storm-scale  
33 conditions (circulation above radar level, rotational velocity, circulation diameter, etc). Elsner  
34 and Schroder (2019) extend this model by making use of the cumulative logistic link function  
35 that estimates probabilities for each damage rating using storm-relative helicity, bulk shear, and  
36 convective available potential energy (CAPE). These studies put statistical guidance for estimating  
37 severe weather outbreak characteristics on a firm mathematical foundation (Cohen et al. 2018;  
38 Elsner and Schroder 2019). Room for additional work in this area motivates the present study. For  
39 instance, the cumulative logistic regression (Elsner and Schroder 2019) provides a distribution for  
40 the *percentage* of tornadoes within each Enhanced Fujita (EF) rating category (Fujita 1981), but a  
41 model is needed to estimate the overall number of tornadoes given the likelihood of at least some  
42 tornadoes.

43 Tornado outbreaks pose a risk of significant loss of life and property. Anderson-Frey and Brooks  
44 (2019) consider the role environmental factors play in the number of outbreak fatalities. They  
45 use self-organizing maps on the significant tornado parameter (STP) and find that more damaging

46 tornadoes (>EF3) present a higher risk for fatalities. However, they also note that both deadly and  
47 non-deadly tornadoes are associated with high values of STP. Self-organizing maps are useful for  
48 describing the role of environmental variables on casualties, but a statistical model is needed to  
49 quantify the relationship between casualty counts and environmental factors. Here we demonstrate  
50 a method to model ‘outbreak’-level tornado and casualty counts from environmental conditions  
51 and predefined tornado clusters. A cluster is defined (informally) as a group of ten or more  
52 tornadoes occurring over a relatively short time scale (e.g., one day) and over a relatively limited  
53 spatial domain (e.g., one to three states) (Fig. 1). The model allows us to quantify the associative  
54 relationships between environmental variables and tornado counts. Moreover, the approach might  
55 eventually help extend the available statistical guidance for predicting outbreak characteristics  
56 particularly when combined with other models.

57 In this paper, we focus on outbreaks rather than on individual tornadoes. The larger space  
58 and time scales associated with the outbreak matches our interest in the larger-scale environmental  
59 factors like CAPE and shear. In what follows, we call the outbreaks ‘clusters’ as is done in Schroder  
60 and Elsner (2019) because we make no attempt to associate the cluster with a particular weather  
61 system. We do not reference the weather feature(s) responsible for the cluster although it is likely  
62 that many of them are associated with a single synoptic-scale system.

63 Clusters in the United States are most frequent during April, May, and June (Dixon et al. 2014;  
64 Tippett et al. 2012; Dean 2010) with most of them occurring across the Central Plains and the  
65 Southeast. Clusters are less common in the Southeast and the Southern Plains during the summer  
66 months as the jet stream migrates north taking the necessary wind shear with it (Concannon et al.  
67 2000; Gensini and Ashley 2011; Jackson and Brown 2009). The percentage of all tornadoes  
68 occurring in clusters has recently been found to be increasing over time (Moore 2017; Tippett et al.  
69 2016; Elsner et al. 2015; Brooks et al. 2014).

70 This paper has two objectives: (1) demonstrate that environmental conditions prior to the  
71 occurrence of any tornadoes can be used to skillfully model the number of tornadoes in a cluster  
72 containing at least ten tornadoes (tornado-count model), and (2) show that these same environmental  
73 conditions can be used to estimate the number of casualties if the number of people in harm's  
74 way is known (casualty-count model). We accomplish these objects by fitting negative binomial  
75 regressions to cluster-level data including environmental variables and tornado and casualty counts  
76 on a convective day (24-hour period between 12 UTC and 12 UTC) when the number of tornadoes  
77 is at least ten [see Elsner and Schroder (2019)]. The paper is outlined as follows. The data and  
78 methods are discussed in section 2 including the mathematics of a negative binomial regression.  
79 Statistics describing the response (i.e., tornado-casualty counts) and environmental variables are  
80 given in section 3. The modeling results are presented in section 4, and a summary with conclusions  
81 are given in section 5.

## 82 **2. Data and methods**

83 We fit regression models to a set of tornado and reanalysis data aggregated to the level of tornado  
84 clusters. Here, we describe how we organize the data and the procedures to aggregate values to the  
85 cluster level. For our purposes, a cluster is a group of at least ten tornadoes occurring relatively  
86 close to one another in both space and time between over a convective day. Ten is chosen as a  
87 compromise between too few clusters leading to greater uncertainty and too many clusters leading  
88 to excessive time required to fit the models (Elsner and Schroder 2019). Ten is also the number  
89 that is sometimes used formally to define an outbreak (Galway 1977; Anderson-Frey et al. 2018).  
90 The number of tornadoes in each cluster is the response variable in the tornado-count regression  
91 model, and the number of casualties is the response variable in the casualty-count regression model.

92 Explanatory variables include outbreak size and location as well as environmental variables from  
93 reanalysis data representing conditions before the occurrence of the first tornado in the cluster.

#### 94 *a. Tornado clusters*

95 First, we extract the date, time, genesis location, and magnitude of all tornado reports between  
96 1994 and 2018 from the Storm Prediction Center [SPC] ([https://www.spc.noaa.gov/gis/  
97 svrgis/](https://www.spc.noaa.gov/gis/svrgis/)). We choose 1994 as the start year because it is the first year of the extensive use of the  
98 WSR-88D Radar (Heiss et al. 1990). In total, there are 30,497 national tornado reports during  
99 this period. The geographic coordinates for each genesis location are converted to Lambert conic  
100 conformal coordinates, where the projection is centered on 96° W longitude.

101 Next, we assign to each tornado a cluster identification number based on the space and time  
102 differences between genesis locations. Two tornadoes are assigned the same cluster identification  
103 number if they occur close together in space and time (e.g., 1 km and 1 h). When the difference  
104 between individual tornadoes and existing clusters surpasses 50,000 s ( $\sim 14$  h), the clustering ends.  
105 The space-time differences have units of seconds because we divide the spatial distance by  $15 \text{ m s}^{-1}$   
106 to account for the average speed of tornado-producing storms. This speed is commensurate with  
107 the magnitude of the steering-level wind field across the clusters. The clustering is identical to  
108 that used in Elsner and Schroder (2019) who developed a cumulative logistic model to the damage  
109 scale at the individual tornado level. Additional details on the procedure, as well as a comparison  
110 of the identified clusters to well-known outbreaks, are available in Schroder and Elsner (2019).

111 We keep only clusters having at least ten tornadoes occurring within the same convective day,  
112 which results in 768 clusters with a total of 17,069 tornadoes. The average number of tornadoes  
113 per cluster is 22 and the maximum is 173 (April 27, 2011). There are 80 clusters with exactly  
114 ten tornadoes. Each cluster varies by area and by where it occurs geographically (see Fig. 1 for

115 examples of clusters). The cluster area is defined by the minimum convex hull (black polygon)  
116 that includes all the tornado genesis locations. The July 19, 1994 cluster with nine tornadoes over  
117 northern Iowa and one over northwest Wisconsin had an area of 33,359 km<sup>2</sup> and lasted about four  
118 hours. The April 27, 2011 cluster had 173 tornadoes spread over more than a dozen states and  
119 had an area of 1,064,337 km<sup>2</sup> with tornadoes occurring throughout the 24-h period (12-UTC to  
120 12-UTC).

121 For each cluster, we sum the number of injuries and deaths across all tornadoes to get the cluster-  
122 level number of casualties (sum of injuries and fatalities). Further, we estimate the population  
123 within the cluster area and the geographic center of the cluster. Population values are U.S. Census  
124 Bureau estimates in cities with at least 40,000 people (Steiner 2019). Population is used as an  
125 explanatory variable in place of cluster area in the casualty-count model.

126 We encountered situations where there were multiple clusters on a given day. For example, there  
127 were two clusters on November 11, 1995 (Fig. 2). The first cluster was responsible for 15 tornadoes  
128 resulting in three casualties. The second cluster was responsible for 10 tornadoes resulting in four  
129 casualties. Both clusters were the result of a single cold front along the eastern coast of the United  
130 States. However, they are not grouped into a single cluster because the minimum between-tornado  
131 space-time distance was larger than our threshold.

### 132 *b. Environmental variables*

133 Large-scale environmental conditions for producing tornadoes are well studied and include large  
134 magnitudes of convective available potential energy, bulk shear, and weak convective inhibition  
135 (Brooks et al. 1994; Rasmussen and Blanchard 1998; Thompson et al. 2003; Shafer and Doswell  
136 2011; Doswell et al. 2006). We obtain variables associated with these environmental condi-  
137 tions from the National Centers for Atmospheric Research's North American Regional Reanalysis

138 (NARR), which is supported by the National Centers for Environmental Prediction (Mesinger et al.  
139 2006). Each variable has numeric values given on a 32-km raster grid with the values available  
140 in three-hour increments starting at 00 UTC. In the severe weather literature, these environmen-  
141 tal variables are called ‘parameters’. However here, since we employ statistical models, we call  
142 them variables to be consistent with the statistical literature where the word ‘parameter’ denotes  
143 unknown model coefficients and moments of statistical distributions (e.g., the mean).

144 We select environmental variables at the nearest three-hour NARR time *prior* to the occurrence  
145 of the first tornado in the cluster. For example, we use the environmental variables given at 15 UTC  
146 if the first tornado in a cluster occurs at 16:30 UTC. This selection criteria results in a sample of the  
147 environment that is less contaminated by the deep convection itself but at a cost that underestimates  
148 the severity in cases where environmental conditions rapidly change favoring tornado development.  
149 About 60% of all clusters have the initial tornado occurring between 18 and 00 UTC (Table 1).  
150 However, there are more tornadoes in clusters when the first tornado occurs between 15 and 18  
151 UTC on average.

152 The environmental variables we consider include convective available potential energy (CAPE)  
153 and convective inhibition (CIN) as computed using the near-surface layer (0 to 180 mb above the  
154 ground level) consistent with Allen et al. (2015b). We also include deep (1000 to 500 mb) and  
155 shallow (1000 to 850 mb) layer bulk shears (DLBS, SLBS) computed as the square root of the sum  
156 of the squared differences between the  $u$  and  $v$  wind components at the respective levels consistent  
157 with Tippett et al. (2012). Climate researchers use these NARR variables at the climatological  
158 scale as proxies for the more traditional variables used in forecasting severe weather (Allen et al.  
159 2015b; Moore et al. 2016; Tippett et al. 2012).

160 We take the highest (lowest for CIN) value across the grid of values within the area defined by the  
161 cluster’s convex hull (Fig. 3). This is done to capture environmental conditions that represent the



162 unadulterated pre-tornado environment. In contrast, the mean (or median) value is influenced by  
163 conditions throughout the domain including earlier occurring non-tornado-producing convection  
164 and in areas within the clusters that did not experience tornado activity. Histograms of the  
165 maximums (not shown) show no evidence of extreme behavior.

166 We do not include storm-relative helicity (SRH), lifted condensation level (LCL), or dewpoint  
167 temperature (DEW) in this research although these variables have proven to be indicators of  
168 favorable environments for tornado production. Storm-relative helicity is not used because it is  
169 correlated with DLBS and SLBS (Table 2). Likewise dew-point temperature and LCL height  
170 are not used because of their relatively high correlation with CAPE. A model that included SRH,  
171 DEW, and LCL height as predictors showed no significant improvement over a model without them.  
172 Further, we do not use composite variables including the significant tornado parameter (STP) and  
173 the supercell composite parameter (SCP). STP, for example, is the product of variables including  
174 CAPE, storm-relative helicity, CIN, and lifted condensation level (LCL) height. A moderate value  
175 of STP can result from either high CAPE and low shear or low CAPE and high shear environments  
176 holding the other variables constant. Here we separate this composite relationship to examine the  
177 direct relationships between CAPE and shear on tornado activity at the scale of outbreaks.

### 178 *c. Negative binomial regression*

179 We fit a negative binomial regression model to the cluster-level data. We chose this type of  
180 regression because the response variable in the tornado (and casualty) model is a count. A count  
181 variable is described by a discrete distribution like the Poisson or negative binomial rather than by  
182 a continuous distribution like the Normal (Gaussian). The choice of which discrete distribution  
183 is made in favor of the negative binomial since the mean number of tornadoes (casualties) per

184 cluster is substantially smaller than the variance in the number of tornadoes (casualties), whereas  
 185 the Poisson distribution assumes the mean is equal to the variance.

186 With the cluster as our unit of analysis, we fit a series of negative binomial regression models to  
 187 the data having the form

$$\begin{aligned}
 T &\sim \text{NegBin}(\hat{\mu}, n) \\
 \ln(\hat{\mu}) &= \beta_0 + \beta_A A + \beta_\phi \phi + \beta_\lambda \lambda + \beta_Y Y + \\
 &\quad \beta_{CAPE} CAPE + \beta_{CIN} CIN + \beta_{DLBS} DLBS + \beta_{SLBS} SLBS,
 \end{aligned}
 \tag{1}$$

188 where the number of tornadoes ( $T$ ) is the dependent variable that is assumed to be adequately  
 189 described by a negative binomial distribution (NegBin) with a rate parameter  $\mu$  and a size parameter  
 190  $n$  (Hilbe 2011). The natural logarithm of the rate parameter is linearly related to cluster area ( $A$ ),  
 191 cluster center location [latitude ( $\phi$ ) and longitude ( $\lambda$ )], year ( $Y$ ) and the four environmental variables  
 192 (CAPE, CIN, DLBS, and SLBS). These are the explanatory variables. The model is fit using the  
 193 method of maximum likelihoods carried out in the call to the `glm.nb` function from MASS package  
 194 in R (Venables and Ripley 2002). We do the same for the initial casualty-count model, but we  
 195 replace cluster area with population ( $P$ ). We simplify the initial models through single-term  
 196 deletions as described in §4.

197 Regression model skill is evaluated by comparing the observed tornado and casualty counts with  
 198 what is predicted by the model. The predicted rates for each cluster are obtained by plugging the  
 199 values of the associated explanatory variables into the model. Predicted rates are under dispersed  
 200 (lower variation) relative to the observed counts. Comparisons are made using the metrics of  
 201 Pearson correlation coefficient and mean absolute error. Predictive skill using these metrics is  
 202 evaluated using in-sample and out-of-sample predictions. In-sample predictions are made using  
 203 all clusters to fit a single model while out-of-sample predictions are made by successively holding

204 one cluster out of the model fitting procedure and using the particular model to predict the counts  
205 from the cluster left out [hold-one-out cross validation; see Elsner and Schmertmann (1994)].

### 206 **3. Results**

#### 207 *a. Descriptive statistics*

208 The number of clusters decreases exponentially with an increasing number of tornadoes per  
209 cluster (Fig. 4). There are 80 clusters with ten tornadoes but only ten clusters with 30 tornadoes.  
210 The right tail of the count distribution is long with the April 27, 2011 cluster having 173 tornadoes  
211 [47 (6%) of the clusters have more than 50 tornadoes and are not shown]. However, more clusters  
212 have 20 or 21 tornadoes than expected from a simple decay function. This deviation is unlikely  
213 the result of physical processes, and it appears too large to be sampling variability. It might be  
214 due to a consistent rounding of the totals to the nearest five or ten. There is an upward trend in  
215 the number of tornadoes per cluster (not shown) consistent with recent studies (Elsner et al. 2015).  
216 The distribution of casualties is also skewed toward many clusters having only a few casualties and  
217 a few have many. Thirty-six percent of all clusters (275) are without a casualty and 56% of the  
218 clusters have fewer than four casualties.

219 There is a seasonality to the chance of at least one tornado cluster (Fig. 5). The empirical  
220 seven-day probability of at least one cluster is between 20 and 30% for much of the year except  
221 between the middle of March and early July (Fig. 5A). The probabilities approach 80% between  
222 mid and late May. The number of tornadoes per cluster is less variable ranging between about 10  
223 and 35 tornadoes per week with no strong seasonality although clusters during July and August  
224 tend to have somewhat fewer tornadoes (Fig. 5B). The casualty rate, defined as the number of

casualties per 100,000 people within the cluster area, has a distinct seasonality with rates being highest between March to April and August to September (Fig. 5C).

Across the 768 clusters the mean of the maximum values of CAPE is  $2,225 \text{ J kg}^{-1}$  and the mean of the minimum values of CIN is  $-114 \text{ J kg}^{-1}$  (Table 3). The maximum deep-layer bulk shear values range from  $5.6$  to  $47.9 \text{ m s}^{-1}$ . Cluster areas range from  $361$  to  $1,064,337 \text{ km}^2$  with an average of  $167,990 \text{ km}^2$ .

### *b. A model for the number of tornadoes*

First, we fit a negative binomial regression to the cluster-level tornado counts using the explanatory variables given in Table 3. This is our tornado-count model. We divide the cluster area by 10 million so it has units of  $100 \text{ km}^2$ . We divide CAPE by 1000 so it has units of  $1000 \text{ J kg}^{-1}$  and we divide CIN by 100 so it has units of  $100 \text{ J kg}^{-1}$ . This simplifies interpretation of the model coefficients, but does not affect the goodness of fit.

All terms have signs on the coefficient that are physically reasonable (Table 4). The number of tornadoes in a cluster increases with cluster area, CAPE, and bulk shear (deep and shallow layers) and increases for decreasing CIN (i.e., less inhibition) as expected. The significance of the variable in statistically explaining tornado counts is assessed by the corresponding  $z$ -value given as the ratio of the coefficient estimate to its standard error (S.E.). We reject the null hypothesis that a particular variable has no explanatory power if its corresponding  $p$ -value is less than .01. Here we fail to reject the null hypothesis for the variables latitude, longitude, and year, which indicates that these non-physical variables have a relatively small impact on tornado counts relative to the physical variables given the data and the model. In particular, there is no significant trend over time in the number of tornadoes in these clusters. The only physical variable that is not statistically significant

247 is CIN. This is likely a result of the NARR data being too coarse to adequately represent CIN. We  
248 remove all statistically insignificant variables before fitting a final model.

249 All variables in the final model are significant although the magnitudes of the coefficients have  
250 changed a bit relative to their values in the initial model. The in-sample correlation between the  
251 observed counts and predicted rates is .59 [(0.54, 0.64), 95% uncertainty interval (UI)] (Fig. 6).  
252 We find that the model is not improved by using the average values of these same environmental  
253 variables. The model statistically explains almost 60% of the variation in cluster-level tornado  
254 counts but tends to over predict the number of tornadoes for smaller clusters and slightly under  
255 predict the number of tornadoes for larger clusters. We test the significance of area and find the  
256 model performance decreases by 25% when excluding area from the model. The mean absolute  
257 error between the observed counts and expected rates is 8.6 tornadoes or 5.2% of the range in  
258 observed counts and 9.3% of the range in predicted rates. The out-of-sample errors are quite  
259 similar due to the large sample size (768 clusters). A hold-one-out cross validation exercise (Elsner  
260 and Schmertmann 1994) results in an out-of-sample correlation of .58 and a mean absolute error  
261 of 8.6 tornadoes. The lag-1 temporal autocorrelation in cluster-level tornado counts is .13.

262 The value of  $\beta_0$  (Table 4) is the regression estimate when all variables in the model are evaluated at  
263 zero. The effect size for a given explanatory variable is given by the magnitude of its corresponding  
264 coefficient. The coefficient is expressed as the difference in the logarithm of the expected tornado  
265 counts for a unit increase in the explanatory variable holding the other variables constant. For  
266 example, the scaled units of CAPE are  $1000 \text{ J kg}^{-1}$ . An increase in CAPE of  $1000 \text{ J kg}^{-1}$  results in  
267 a  $(\exp(.0459) - 1) \times 100\% = 4.7\%$  increase in the expected number of tornadoes, conditional on at  
268 least ten tornadoes. Continuing, units of deep-layer bulk shear are  $10 \text{ m s}^{-1}$  so an increase in shear  
269 of  $10 \text{ m s}^{-1}$  results in a 13% increase in the expected number of tornadoes. A similar increase in  
270 shallow-layer bulk shear results in a 11.1% increase in the number of tornadoes.

271 Changes to the expected number of tornadoes given changes in the environmental variables  
 272 have a large impact on the probability distribution of counts conditional on the cluster area. The  
 273 negative binomial distribution for the number of tornadoes  $T$  with an expected number of tornadoes  
 274  $\bar{T}$  (obtained from the regression model) has a probability density

$$\Pr(T = k) = \frac{\Gamma(r + k)}{k! \Gamma(r)} \left( \frac{r}{r + \bar{T}} \right)^r \left( \frac{\bar{T}}{r + \bar{T}} \right)^k \quad \text{for } k = 10, 11, 12, \dots, \quad (2)$$

275 where  $r = 1/n$  and  $\Gamma(z) = \int_0^\infty x^{z-1} e^{-x} dx$  is the gamma function.

276 For example, on April 12, 2020 the 12 UTC guidance from the SPC convective outlook defined an  
 277 area with a 10% chance of at least one tornado occurring within 40 km of any location (10% tornado  
 278 risk). The area of the polygon was approximately 400,000 km<sup>2</sup> (much larger than the average cluster  
 279 area) centered on Mississippi (Fig. 7). With an area of that size, the model estimates the probability  
 280 of at least 30 tornadoes for a range of deep-layer shear values and conditional on the amount of  
 281 CAPE while holding shallow-layer shear at the average value of all clusters (Fig. 8). Given an  
 282 average amount of shallow-layer shear, a deep-layer shear of 10 m s<sup>-1</sup> and low CAPE (5th percentile  
 283 value), the model predicts a 17% [9, 26%, UI] chance of at least 30 tornadoes (given a cluster with  
 284 at least ten tornadoes). In contrast, given a deep-layer shear of 40 m s<sup>-1</sup> and high CAPE (95th  
 285 percentile value), the model predicts a 65% [(56, 71%), UI] chance of at least 30 tornadoes. There  
 286 were more than 100 tornadoes on that day.

287 The model quantifies the empirical relationship between CAPE and, independently, shear in  
 288 terms of a probability distribution on the number of tornadoes. It predicts the expected count  
 289 given values for the explanatory variables. The negative binomial distribution uses the model's  
 290 predicted count and the size parameter to generate a distribution of probabilities. For example, the  
 291 model gives predicted probabilities across a range of CAPE and deep-layer shear values (holding  
 292 shallow-layer shear at its mean value) that provides a picture of the relationship (Fig. 9). The

293 predicted probabilities of at least 30 tornadoes given an outbreak covering an area of 400,000 km<sup>2</sup>  
294 increase from low values of both CAPE and shear to high values of both CAPE and shear.

295 *c. Sensitivity of the results to cluster definition*

296 The clustering methodology is taken from Schroder and Elsner (2019) where a sensitivity analysis  
297 was performed to examine the reliability of the resulting clusters. They examined various stopping  
298 thresholds and determined that a space-time distance of 5000 s best matched the subjectively  
299 identified outbreaks of Forbes (2006) with an agreement of 88%. Larger and smaller stopping  
300 thresholds resulting in lower agreement percentages. Still this objective method results in clusters  
301 with varying levels of tornado density (tornadoes per unit area), which might influence the results  
302 of the regression model. For example, Fig. 1 shows that the June 6, 1999 cluster has much lower  
303 tornado density compared to the February 5, 2008 cluster.

304 To directly test the sensitivity of our cluster definition, we first correlate the model residuals  
305 (observed count minus the predicted rate) for each cluster with the tornado density. The Pearson  
306 product-moment correlation coefficient is .02 indicating that tornado density is not a significant  
307 factor in the model's ability to predict the conditional tornado counts from the environmental  
308 variables. Second, we refit the model using all clusters except the five clusters having the lowest  
309 tornado density. The mean absolute error is only marginally improved from 8.6 to 8.4 tornadoes,  
310 providing further evidence that model results are not particularly sensitive to the inclusion of  
311 clusters with low tornado density.

312 *d. A model for the number of casualties*

313 Next we fit a negative binomial regression to the cluster-level casualty counts (direct injuries and  
314 deaths) using the same explanatory variables (Table 3) with the exceptions that population (scaled

315 by 100,000 residents) replaces cluster area and  $C$  (casualty count) replaces  $T$  (tornado count) as  
316 the dependent variable. This is our casualty-count model. We find that CIN is the only variable  
317 not significant in the initial model (Table 5). We remove it before fitting a final model.

318 The in-sample correlation between the observed casualty counts and predicted rates is .43 [(0.37,  
319 .48), 95% UI] (Fig. 10). We test the significance of population and find the model performance  
320 decreases by 12% when excluding population from the model. The mean absolute error between  
321 the observed counts and expected rates is 39 casualties or 1.3% of the range in observed counts and  
322 3.4% of the range in predicted rates. The out-of-sample correlation is .36 and the mean absolute  
323 error is 40 casualties. The skill is lower than the skill of the tornado-count model as there is  
324 additional uncertainty associated with the number of casualties given a tornado. The lower skill is  
325 also a result of the many other factors that can influence casualties including demographic variables  
326 and location (see Summary and Conclusions).

327 As expected from the tornado-count model, the number of casualties resulting from a cluster of  
328 tornadoes increases with CAPE and with the two bulk shear variables (Table 5) which is consistent  
329 with Anderson-Frey and Brooks (2019). Holding all other variables constant, an increase in CAPE  
330 of  $1000 \text{ J kg}^{-1}$  results in a 28% increase in the expected number of casualties. An increase in  
331 deep-layer bulk shear of  $10 \text{ m s}^{-1}$  results in a 98% increase in the expected number of casualties  
332 per cluster and a similar increase in shallow-layer bulk shear results in a 76% increase in the  
333 expected number of casualties per cluster, conditional on at least ten tornadoes. Additionally, the  
334 model indicates that casualties decrease at a rate of 3.6% per year. This is very likely the result of  
335 improvements made by the National Weather Service in warning coordination and dissemination  
336 leading to better awareness especially for these large outbreak events.

337 Also, as expected, the number of people in harm's way is a significant explanatory variable for  
338 the cluster-level casualty count. The relationship between population and number of casualties is



339 quantified at the tornado-level in Elsner et al. (2018) and Fricker et al. (2017) so we expect the  
340 relationship to hold at the cluster level. Here, we are able to compare the influence of shear and  
341 CAPE on the probability of casualties as modulated by population (Fig. 11). Model results are  
342 shown for three levels of population. The probability of a large number of casualties increases with  
343 increasing shear and increasing CAPE, while keeping the other variables at their mean values and  
344 year at 2018.

345 Importantly, we also find that where the cluster occurs has a significant influence on the number  
346 of casualties consistent with other studies (Ashley and Strader 2016; Fricker and Elsner 2019).  
347 For every one degree north latitude, the casualty rate decreases by 5.5% and for every one degree  
348 east longitude the casualty rate increases by 2.9%. Thus, cluster-level casualties are highest over  
349 the Southeast. This effect is independent of the number of tornadoes since location was not a  
350 significant factor in the tornado-count model. The result is also independent of the number of  
351 people in harm's way since population is included as an exploratory variable in the model.

352 To visualize the difference of the combined effects of latitude and longitude on the difference in  
353 the probability of many casualties, we plot modeled casualty probabilities (at least 25) as a function  
354 of CAPE and deep-layer shear for two *hypothetical* outbreaks that are the same in every way except  
355 one outbreak is centered on Sioux City, Iowa (42.5° N, 96.4° W), and the other is centered on  
356 Birmingham, Alabama (33.5° N, 86.8° W) (Fig. 12). The modeled probabilities are lowest (around  
357 5%) for low CAPE and shear values and highest (above 30%) for high CAPE and shear values.  
358 The difference in modeled probabilities across these two locations peaks at about +12 percentage  
359 points for high CAPE and high shear regimes when the outbreak is centered on Birmingham.

#### 360 **4. Summary and conclusions**

361 Estimating characteristics of severe weather outbreaks (e.g., tornado and casualty counts) is  
362 challenging but important. Forecasters use a combination of numerical weather prediction and  
363 empirical guidance to outline areas of severe convective weather. Here, we demonstrate a statistical  
364 regression model that can take advantage of the large sample of independent tornado ‘outbreaks’ as  
365 a way to statistically explain the number of tornadoes and the number of casualties in a cluster of at  
366 least ten tornadoes. We fit negative binomial regressions to tornado characteristics aggregated to  
367 the level of tornado clusters where a cluster is a space-time group of at least ten tornadoes occurring  
368 between 12 UTC and 12 UTC over the period 1994–2018. The number of tornadoes in each cluster  
369 is the response variable in the tornado-count model, and the number of casualties (deaths plus  
370 injuries) is the response variable in the casualty-count model. Environmental explanatory variables  
371 for the models are extracted from reanalysis data representing conditions before the occurrence of  
372 the first tornado in the cluster consistent with Schroder and Elsner (2019). Additional explanatory  
373 variables include cluster area, population, location, and year.

374 The estimated tornado rates, conditional on there being at least ten tornadoes, explain 59% of the  
375 observed tornado counts in-sample, and the estimated casualty rates explain 43% of the observed  
376 casualty counts in-sample. Because of the large sample size, the out-of-sample skill is lower but  
377 still useful. The models show that a  $1000 \text{ J kg}^{-1}$  increase in CAPE results in a 4.7% increase in  
378 the expected number of tornadoes conditional on at least ten tornadoes and a 28% increase in the  
379 expected number of casualties, holding the other variables constant. The models further show that  
380 a  $10 \text{ m s}^{-1}$  increase in deep-layer bulk shear results in a 13% increase in the expected number of  
381 tornadoes and a 98% increase in the expected number of casualties, holding the other variables  
382 constant. This research is consistent with Anderson-Frey and Brooks (2019) who found the number

383 of tornadoes and casualties to increase with both CAPE and shear. This study quantifies these  
384 increases. The casualty-count model also shows a significant decline in the number of casualties  
385 at a rate of 3.6% per year. Casualty rates depend on where the outbreak occurs with more deaths  
386 and injuries, on average, over the Southeast, controlling for the other variables; a result that is  
387 consistent with the recent work of Fricker and Elsner (2019) and Biddle et al. (2020).

388 Some of the unexplained variability in cluster-level tornado counts (and casualty counts) arises  
389 from the uncertainty associated with the preferred storm mode and the evolution of meso-scale  
390 convective systems, neither of which are captured by a single maximum value in the variable space  
391 of CAPE and shear. The counts are also limited by the quality of the NARR data. The NARR  
392 tends to unrealistically favor tornado environments during specific convective setups (Gensini and  
393 Ashley 2011; Gensini et al. 2014; Allen et al. 2015a). Additionally, we use only the maximum  
394 values (minimum for CIN) of the environmental variables which may limit the representation of  
395 the cluster environment. Also, outbreaks associated with tropical cyclones likely add a bit of noise  
396 to both models since the number of tornadoes is sensitive to the extent and location of convective  
397 bursts within overall evolution of the land-falling storm.

398 The casualty-count model would be improved by including a skillful estimate of the number  
399 of tornadoes. Indeed in a perfect-prognostic setting, where we know the number of tornadoes in  
400 the outbreak, the out-of-sample correlation between the observed number of casualties and the  
401 modeled estimated rate of casualties increases to .79. Further, although our approach to extracting  
402 signal from noise in the tornado dataset is sound, exclusive focus on clusters with at least ten  
403 tornadoes is a type of selection bias meaning that the sample of data used to fit the model does not  
404 represent the population of all outbreaks, which limits what we can say in general about the effect  
405 of convective environments on the probability distribution of casualty counts.

406 The tornado-count model can be modified to provide guidance to forecasters given a convective  
407 outlook that highlights an area of elevated threat for tornadoes and a prediction of CAPE and  
408 shear across the threat area. The model needs to be calibrated using threat polygons (not cluster  
409 areas as was done here) and include *predicted* environmental values, but the same model equation  
410 can be used to provide a forecast probability distribution on the number of tornadoes. Further, a  
411 numerical convolution of this probability distribution with a forecast probability distribution for  
412 each EF-rating category (Elsner and Schroder 2019) will result in a prediction of the expected  
413 number of counts by category as well as the associated uncertainties.

414 The casualty-count model can be employed in a research setting to help better understand the  
415 socioeconomic, demographic, and communication factors that make some communities particularly  
416 vulnerable to deaths and injuries (Dixon and Moore 2012; Senkbeil et al. 2013; Klockow et al.  
417 2014; Fricker and Elsner 2019). Work along this line has been done at the individual tornado  
418 level by identifying unusually devastating events (Fricker and Elsner 2019), but scaling this type  
419 of analysis to the cluster-level to identify unusually devastating outbreaks might provide additional  
420 insights.

421 Finally, it is possible that the models could be improved by including nonlinear effects. One type  
422 of non-linearity is interaction where the effect of CAPE on casualties is modulated by shear, for  
423 example. However, interaction effects usually must be specified without reference to the data, so  
424 additional research on this is needed. The model could also be improved by including variables  
425 that represent other environmental factors, convective modes, and efficiency of tornado production.  
426 The models also might be improved by adjusting the threshold definition of a cluster. Increasing  
427 the threshold on the tornado-count model from 10 to 14 decreases the sample size to 505 clusters  
428 and reduces the effect sizes on CAPE and shear by around 25%. Decreasing the threshold from 10  
429 to 6 increases the sample size and, thus, reduces the standard error assuming the effect size stays

430 the same. A casualty-count model might also be improved by relaxing the assumption that the  
431 numbers of people injured or killed are independent. Casualty counts are typically not independent  
432 at the household level where multiple people live under the same roof. In this case a better model  
433 might include a zero-inflated count process.

434 *Acknowledgments.* The negative binomial regression models in this paper were implemented with  
435 the `glm.nb` function from the MASS R package (Venables and Ripley 2002). Graphics were made  
436 with the `ggplot2` framework (Wickham 2017). The code and data to fit all the models is available  
437 on GitHub (<https://github.com/jelsner/cape-shear>).

## References

- Allen, J. T., M. K. Tippett, and A. H. Sobel, 2015a: An empirical model relating U.S. monthly hail occurrence to large-scale meteorological environment. *Journal of Advances in Modeling Earth Systems*, **7** (1), 226–243, doi:10.1002/2014MS000397, URL <https://agupubs.onlinelibrary.wiley.com/doi/abs/10.1002/2014MS000397>.
- Allen, J. T., M. K. Tippett, and A. H. Sobel, 2015b: Influence of the El Niño/Southern Oscillation on tornado and hail frequency in the United States. *Nature Geosciences*, **8**, 278–283.
- Anderson-Frey, A. K., and H. Brooks, 2019: Tornado fatalities: An environmental perspective. *Weather and Forecasting*, **34** (6), 1999–2015, doi:10.1175/waf-d-19-0119.1, URL <https://doi.org/10.1175/waf-d-19-0119.1>.
- Anderson-Frey, A. K., Y. P. Richardson, A. R. Dean, R. L. Thompson, and B. T. Smith, 2018: Near-storm environments of outbreak and isolated tornadoes. *Weather and Forecasting*, **33** (5), 1397–1412, doi:10.1175/WAF-D-18-0057.1, URL <https://doi.org/10.1175/WAF-D-18-0057.1>, <https://doi.org/10.1175/WAF-D-18-0057.1>.
- Ashley, W. S., and S. M. Strader, 2016: Recipe for disaster: How the dynamic ingredients of risk and exposure are changing the tornado disaster landscape. *Bulletin of the American Meteorological Society*, **97**, 767–786.
- Biddle, M. D., R. P. Brown, C. A. Doswell, and D. R. Legates, 2020: Regional differences in the human toll from tornadoes: A new look at an old idea. *Weather, Climate, and Society*, **12** (4), 815–825, doi:10.1175/wcas-d-19-0051.1, URL <https://doi.org/10.1175/wcas-d-19-0051.1>.
- Brooks, H. E., G. W. Carbin, and P. T. Marsh, 2014: Increased variability of tornado occurrence in the United States. *Science*, **346** (6207), 349–352, doi:10.1126/science.1257460, URL

460 <https://science.sciencemag.org/content/346/6207/349>, [https://science.sciencemag.org/content/](https://science.sciencemag.org/content/346/6207/349.full.pdf)  
461 [346/6207/349.full.pdf](https://science.sciencemag.org/content/346/6207/349.full.pdf).

462 Brooks, H. E., C. A. Doswell , and J. Cooper, 1994: On the environments of tornadic and  
463 nontornadic mesocyclones. *Weather and Forecasting*, **9**, 606–618, doi:10.1175/1520-0434.

464 Cohen, A. E., J. B. Cohen, R. L. Thompson, and B. T. Smith, 2018: Simulating tornado probability  
465 and tornado wind speed based on statistical models. *Weather and Forecasting*, **33** (4), 1099–1108,  
466 doi:10.1175/waf-d-17-0170.1, URL <https://doi.org/10.1175/waf-d-17-0170.1>.

467 Concannon, P., H. E. Brooks, and C. A. Doswell , 2000: Climatological risk of strong and violent  
468 tornadoes in the United States. *Second Conference on Environmental Applications*.

469 Dean, A. R., 2010: P2.19 An analysis of clustered tornado events. *25th Conference on Severe Local*  
470 *Storms*.

471 Dixon, P. G., A. E. Mercer, K. Grala, and W. H. Cooke, 2014: Objective identification of tornado  
472 seasons and ideal spatial smoothing radii. *Earth Interactions*, **18**, 1–15.

473 Dixon, R. W., and T. W. Moore, 2012: Tornado vulnerability in Texas. *Weather, Climate, and*  
474 *Society*, **4**, 59–68.

475 Doswell, C. A., R. Edwards, R. L. Thompson, J. A. Hart, and K. C. Crosbie, 2006: A simple and  
476 flexible method for ranking severe weather events. *Weather and Forecasting*, **21** (6), 939–951,  
477 doi:10.1175/waf959.1, URL <https://doi.org/10.1175/waf959.1>.

478 Elsner, J. B., S. C. Elsner, and T. H. Jagger, 2015: The increasing efficiency of tornado days in the  
479 United States. *Climate Dynamics*, **45** (3-4), 651–659.

- 480 Elsner, J. B., T. Fricker, and W. D. Berry, 2018: A model for U.S. tornado casualties involving  
481 interaction between damage path estimates of population density and energy dissipation. *Journal*  
482 *of Applied Meteorology and Climatology*, **57**, 2035–2046.
- 483 Elsner, J. B., and C. P. Schmertmann, 1994: Assessing forecast skill through cross validation.  
484 *Weather and Forecasting*, **9** (4), 619–624.
- 485 Elsner, J. B., and Z. Schroder, 2019: Tornado damage ratings estimated with cumulative logistic  
486 regression. *Journal of Applied Meteorology and Climatology*, **58** (12), 2733–2741, doi:10.1175/  
487 jamc-d-19-0178.1, URL <https://doi.org/10.1175/jamc-d-19-0178.1>.
- 488 Forbes, G. S., 2006: Meteorological aspects of high-impact tornado outbreaks. Preprints, *22nd*  
489 *Conf. on Severe Local Storms*, Hyannis, MA, Amer. Meteor. Soc., 1–12.
- 490 Fricker, T., and J. B. Elsner, 2019: Unusually devastating tornadoes in the United States:  
491 1995–2016. *Annals of the American Association of Geographers*, **110** (3), 724–738, doi:  
492 10.1080/24694452.2019.1638753, URL <https://doi.org/10.1080/24694452.2019.1638753>.
- 493 Fricker, T., J. B. Elsner, and T. H. Jagger, 2017: Population and energy elasticity of tornado  
494 casualties. *Geophysical Research Letters*, **44**, 3941–3949, doi:10.1002/2017GL073093.
- 495 Fujita, T. T., 1981: Tornadoes and downbursts in the context of generalized planetary scales. *J.*  
496 *Atmos. Sci.*, **38**, 1511–1534.
- 497 Galway, J. G., 1977: Some climatological aspects of tornado outbreaks. *Monthly Weather Review*,  
498 **105**, 477–484.
- 499 Gensini, V., and W. Ashley, 2011: Climatology of potentially severe convective environments from  
500 the North American Regional Reanalysis. *Electronic Journal of Severe Storms Meteorology*, **6**,  
501 1–40, doi:10.1038/s41612-018-0048-2.



502 Gensini, V. A., T. L. Mote, and H. E. Brooks, 2014: Severe-thunderstorm reanalysis environments  
503 and collocated radiosonde observations. *Journal of Applied Meteorology and Climatology*,  
504 **53** (3), 742–751, doi:10.1175/jamc-d-13-0263.1, URL <https://doi.org/10.1175/jamc-d-13-0263.1>.  
505 1.

506 Heiss, W. H., D. L. McGrew, and D. Sirmans, 1990: NEXRAD: next generation weather radar  
507 (WSR-88D). *Microwave Journal*, **33** (1), 79.

508 Hilbe, J., 2011: *Negative Binomial Regression*. Cambridge University Press.

509 Hill, A. J., G. R. Herman, and R. S. Schumacher, 2020: Forecasting severe weather with random  
510 forests. *Monthly Weather Review*, doi:10.1175/mwr-d-19-0344.1, URL <https://doi.org/10.1175/mwr-d-19-0344.1>.  
511 mwr-d-19-0344.1.

512 Hitchens, N. M., and H. E. Brooks, 2014: Evaluation of the Storm Prediction Center’s convective  
513 outlooks from day 3 through day 1. *Weather and Forecasting*, **29** (5), 1134–1142, doi:10.1175/waf-d-13-00132.1, URL <https://doi.org/10.1175/waf-d-13-00132.1>.  
514 waf-d-13-00132.1.

515 Jackson, J. D., and M. E. Brown, 2009: Sounding-derived low-level thermodynamic characteristics  
516 associated with tornadic and non-tornadic supercell environments in the Southeast United States.  
517 *National Weather Digest*, **33**, 16–26.

518 Klockow, K. E., R. A. Pepler, and R. A. McPherson, 2014: Tornado folk science in Alabama  
519 and Mississippi in the 27 April 2011 tornado outbreak. *GeoJournal*, **79** (6), 791–804, doi:  
520 10.1007/s10708-013-9518-6, URL <https://doi.org/10.1007/s10708-013-9518-6>.

521 Mesinger, F., and Coauthors, 2006: North American Regional Reanalysis. *Bulletin of the American  
522 Meteorological Society*, **87** (3), 343–360, doi:10.1175/BAMS-87-3-343, URL <https://doi.org/10.1175/BAMS-87-3-343>,  
523 10.1175/BAMS-87-3-343, <https://doi.org/10.1175/BAMS-87-3-343>.

- 524 Moore, T., 2017: On the temporal and spatial characteristics of tornado days in the United States.  
525 *Atmospheric Research*, **184**, doi:10.1016/j.atmosres.2016.10.007.
- 526 Moore, T. W., R. W. Dixon, and N. J. Sokol, 2016: Tropical cyclone Ivan's tornado cluster  
527 in the Mid-Atlantic region of the United States on 17–18 September 2004. *Physical Geogra-*  
528 *phy*, **37 (3-4)**, 210–227, doi:10.1080/02723646.2016.1189299, URL [https://doi.org/10.1080/](https://doi.org/10.1080/02723646.2016.1189299)  
529 [02723646.2016.1189299](https://doi.org/10.1080/02723646.2016.1189299).
- 530 Rasmussen, E. N., and D. O. Blanchard, 1998: A baseline climatology of sounding-  
531 derived supercell and tornado forecast parameters. *Weather and Forecasting*, **13 (4)**, 1148–  
532 1164, doi:10.1175/1520-0434(1998)013<1148:ABCOSD>2.0.CO;2, URL [https://doi.org/10.](https://doi.org/10.1175/1520-0434(1998)013<1148:ABCOSD>2.0.CO;2)  
533 [1175/1520-0434\(1998\)013<1148:ABCOSD>2.0.CO;2](https://doi.org/10.1175/1520-0434(1998)013<1148:ABCOSD>2.0.CO;2).
- 534 Schroder, Z., and J. B. Elsner, 2019: Quantifying relationships between environmental factors  
535 and power dissipation on the most prolific days in the largest tornado “outbreaks”. *International*  
536 *Journal of Climatology*, doi:10.1002/joc.6388, URL <https://doi.org/10.1002/joc.6388>.
- 537 Senkbeil, J. C., D. A. Scott, P. Guinazu-Walker, and M. S. Rockman, 2013: Ethnic and racial  
538 differences in tornado hazard perception, preparedness, and shelter lead time in Tuscaloosa. *The*  
539 *Professional Geographer*, **66 (4)**, 610–620, doi:10.1080/00330124.2013.826562, URL [https://](https://doi.org/10.1080/00330124.2013.826562)  
540 [doi.org/10.1080/00330124.2013.826562](https://doi.org/10.1080/00330124.2013.826562).
- 541 Shafer, C. M., and C. A. Doswell, 2011: Using kernel density estimation to identify, rank, and  
542 classify severe weather outbreak events. *Electronic Journal of Severe Storms Meteorology*, **6**,  
543 1–28.
- 544 Steiner, E., 2019: Spatial history project. Center for Spatial and Textual Analysis, Stanford Uni-  
545 versity, URL <http://web.stanford.edu/group/spatialhistory/cgi-bin/site/index.php>.

- 546 Thompson, R. L., R. Edwards, J. A. Hart, K. L. Elmore, and P. Markowski, 2003: Close proxim-  
547 ity soundings within supercell environments obtained from the Rapid Update Cycle. *Weather*  
548 *and Forecasting*, **18** (6), 1243–1261, doi:10.1175/1520-0434(2003)018<1243:cpswse>2.0.co;2,  
549 URL [https://doi.org/10.1175/1520-0434\(2003\)018<1243:cpswse>2.0.co;2](https://doi.org/10.1175/1520-0434(2003)018<1243:cpswse>2.0.co;2).
- 550 Thompson, R. L., and Coauthors, 2017: Tornado damage rating probabilities derived from WSR-  
551 88D data. *Weather and Forecasting*, **32** (4), 1509–1528, doi:10.1175/waf-d-17-0004.1, URL  
552 <https://doi.org/10.1175/waf-d-17-0004.1>.
- 553 Tippett, M. K., C. Lepore, and J. E. Cohen, 2016: More tornadoes in the most extreme U.S.  
554 tornado outbreaks. *Science*, **354** (6318), 1419–1423, doi:10.1126/science.aah7393, URL <https://doi.org/10.1126/science.aah7393>.
- 556 Tippett, M. K., A. H. Sobel, and S. J. Camargo, 2012: Association of U.S. tornado occurrence  
557 with monthly environmental parameters. *Geophysical Research Letters*, **39**, L02 801.
- 558 Venables, W. N., and B. D. Ripley, 2002: *Modern Applied Statistics with S*. 4th ed., Springer, New  
559 York, URL <http://www.stats.ox.ac.uk/pub/MASS4>, ISBN 0-387-95457-0.
- 560 Wickham, H., 2017: *tidyverse: Easily Install and Load 'Tidyverse' Packages*. URL [https://CRAN.](https://CRAN.R-project.org/package=tidyverse)  
561 [R-project.org/package=tidyverse](https://CRAN.R-project.org/package=tidyverse), r package version 1.1.1.

562 **LIST OF TABLES**

563 **Table 1.** Cluster statistics by time of day. Each cluster is categorized by the closest  
564 three-hour time (defined by the NARR data) prior to the first tornado. . . . . 29

565 **Table 2.** Correlation matrix of environmental variables considered in this study. Dew-  
566 point temperature (DEW), specific humidity (SH), and storm relative helicity  
567 (HLCY). Only CAPE, CIN, DLBS, and SLBS are used as explanatory variables  
568 in the models. . . . . 30

569 **Table 3.** Variables considered in the regression models. Values include the range and  
570 average across the 768 tornado clusters. . . . . 31

571 **Table 4.** Coefficients in the tornado-count models. The size parameter ( $n$ ) is  $6.27 \pm .393$   
572 (standard error) for the initial model  $6.25 \pm .392$  (standard error) for the final  
573 model. . . . . 32

574 **Table 5.** Coefficients in the casualty-county models. The size parameter ( $n$ ) is  $.261 \pm .014$   
575 (standard error) for the initial and final models. . . . . 33

576 TABLE 1. Cluster statistics by time of day. Each cluster is categorized by the closest three-hour time (defined  
 577 by the NARR data) prior to the first tornado.

Time of Day (UTC)	Number of Clusters	Number of Tornadoes	Average Tornadoes Per Cluster	Average Duration (hours)
00	33	523	15.8	6.1
03	5	67	13.4	6.4
06	2	23	11.5	3.2
12	145	3598	12.1	14.0
15	124	3222	26.0	11.5
18	249	5220	21.0	8.4
21	210	4416	21.0	7.0

578 TABLE 2. Correlation matrix of environmental variables considered in this study. Dew-point temperature  
 579 (DEW), specific humidity (SH), and storm relative helicity (HLCY). Only CAPE, CIN, DLBS, and SLBS are  
 580 used as explanatory variables in the models.

	CAPE	CIN	DLBS	SLBS	HLCY	DEW	SH
CAPE	1.00						
CIN	-0.07	1.00					
DLBS	-0.03	-0.29	1.00				
SLBS	-0.37	-0.24	0.49	1.00			
HLCY	-0.22	-0.30	<b>0.58</b>	<b>0.76</b>	1.00		
DEW	<b>0.56</b>	0.00	-0.08	0.02	-0.08	1.00	
SH	<b>0.64</b>	0.00	-0.12	-0.08	-0.13	<b>0.98</b>	1.00

581 TABLE 3. Variables considered in the regression models. Values include the range and average across the 768  
 582 tornado clusters.

Variable	Abbreviation	Range	Average
Explanatory Variables			
Convective Available Potential Energy [ $\text{J kg}^{-1}$ ]	CAPE	[0, 6530]	2225
Convective Inhibition [ $\text{J kg}^{-1}$ ]	CIN	[-668, 0]	-114
Deep-Layer Bulk Shear [ $\text{m s}^{-1}$ ]	DLBS	[5.6, 48]	27.5
Shallow-Layer Bulk Shear [ $\text{m s}^{-1}$ ]	SLBS	[1.1, 33.8]	15.0
Latitude [ $^{\circ}$ N]	$\phi$	[27.12, 48.97]	37.20
Longitude [ $^{\circ}$ E]	$\lambda$	[-109.9 -72.88]	-92.16
Cluster Area [ $\text{km}^2$ ]	$A$	[361, 1,064,337]	167,990
Population [No. of People]	$P$	[0, 38,226,946]	3,387,259
Year	$Y$	[1994, 2018]	2006
Response Variables			
Number of Tornadoes	$T$	[10, 173]	22.2
Number of Casualties (injuries plus deaths)	$C$	[0, 3,069]	29.9

583 TABLE 4. Coefficients in the tornado-count models. The size parameter ( $n$ ) is  $6.27 \pm .393$  (standard error) for  
 584 the initial model  $6.25 \pm .392$  (standard error) for the final model.

Coefficient	Estimate	S.E.	$z$ value	$\Pr(> z )$
Initial Model				
$\beta_0$	4.5489	4.7662	0.9540	0.3399
$\beta_A$	0.0146	0.0011	12.80	< 0.0001
$\beta_\phi$	-0.0051	0.0043	-1.17	0.2427
$\beta_\lambda$	-0.0028	0.0031	-0.917	0.3594
$\beta_Y$	-0.0012	0.0024	-0.515	0.6068
$\beta_{CAPE}$	0.0452	0.0153	2.96	0.0031
$\beta_{CIN}$	-0.0110	0.0189	-0.581	0.5612
$\beta_{DLBS}$	0.1256	0.0292	4.30	< 0.0001
$\beta_{SLBS}$	0.1059	0.0355	2.98	0.0029
Final Model				
$\beta_0$	2.1779	0.0817	26.65	< 0.0001
$\beta_A$	0.0149	0.0011	13.85	< 0.0001
$\beta_{CAPE}$	0.0459	0.0146	3.13	0.0017
$\beta_{DLBS}$	0.1254	0.0288	4.35	< 0.0001
$\beta_{SLBS}$	0.1054	0.0314	3.35	0.0008



585 TABLE 5. Coefficients in the casualty-county models. The size parameter ( $n$ ) is  $.261 \pm .014$  (standard error)  
 586 for the initial and final models.

Coefficient	Estimate	S.E.	$z$ value	$\Pr(> z )$
Initial Model				
$\beta_0$	76.6908	20.7430	3.70	0.0002
$\beta_P$	0.0122	0.0019	6.51	< 0.0001
$\beta_\phi$	-0.0561	0.0187	-3.00	0.0027
$\beta_\lambda$	0.0284	0.0136	2.09	0.0363
$\beta_Y$	-0.0364	0.0103	-3.52	0.0004
$\beta_{CAPE}$	0.2436	0.0643	3.79	0.0002
$\beta_{CIN}$	0.0052	0.0802	0.07	0.9479
$\beta_{DLBS}$	0.6853	0.1262	5.43	< 0.0001
$\beta_{SLBS}$	0.5650	0.1534	3.68	0.0002
Final Model				
$\beta_0$	76.7677	20.6902	3.71	0.0002
$\beta_P$	0.0122	0.0018	6.67	0.0000
$\beta_\phi$	-0.0563	0.0186	-3.02	0.0025
$\beta_\lambda$	0.0287	0.0130	2.20	0.0277
$\beta_Y$	-0.0364	0.0103	-3.53	0.0004
$\beta_{CAPE}$	0.2440	0.0643	3.79	0.0001
$\beta_{DLBS}$	0.6833	0.1253	5.45	0.0000
$\beta_{SLBS}$	0.5631	0.1504	3.74	0.0002

587 **LIST OF FIGURES**

588 **Fig. 1.** Example tornado clusters. Each point is the tornadogenesis location shaded by EF rating.  
 589 The black line is the spatial extent of the tornadoes occurring on that convective day and is  
 590 defined by the minimum convex hull encompassing the set of locations. . . . . 36

591 **Fig. 2.** Example of multiple clusters on a single convective day. Each point is a tornado genesis  
 592 location. The black line is the spatial extent of the tornadoes for each cluster and is defined  
 593 by the minimum convex hull encompassing the set of locations . . . . . 37

594 **Fig. 3.** Example of the environmental factors for the May 6, 2003. The black line is the spatial extent  
 595 of the cluster on that convective day. Shading represents the intensity of the environment.  
 596 CAPE is purple, helicity is blue, CIN is green, and deep layer shear is red. The black square  
 597 is the location of the maximum value for the environmental factor. . . . . 38

598 **Fig. 4.** Histograms of the number of clusters by number of tornadoes (A) and number of clusters by  
 599 number of casualties (B). The histograms are right-truncated at 50 to show detail on the left  
 600 side of the distributions. Only clusters with at least ten tornadoes are considered in this study. . . 39

601 **Fig. 5.** Probability of a cluster (A), average number of tornadoes per cluster (B), and average number  
 602 of casualties per 1 000 000 people per cluster (C) by week of the year. . . . . 40

603 **Fig. 6.** Observed cluster-level tornado counts versus predicted rates from a negative binomial re-  
 604 gression. The thin black line is the line of best fit. The thick line is the slope of the  
 605 model indicating the relationship between the observed and predicted tornado counts and the  
 606 associated standard error. . . . . 41

607 **Fig. 7.** Convective outlook issued by the Storm Prediction Center at 12 UTC on April 12, 2020  
 608 and the locations of tornado reports over the 24-hr period starting at that time. The outlook  
 609 category numbers indicate the chance of observing severe weather within 40 km of any  
 610 location. The convective outlook shapefiles are from [www.spc.noaa.gov/cgi-bin-spc/  
 611 getacrange.pl?date0=20200412&date1=20200412](http://www.spc.noaa.gov/cgi-bin-spc/getacrange.pl?date0=20200412&date1=20200412) and the tornado reports are from  
 612 [www.spc.noaa.gov/climo/reports/200412\\_rpts.html](http://www.spc.noaa.gov/climo/reports/200412_rpts.html). . . . . 42

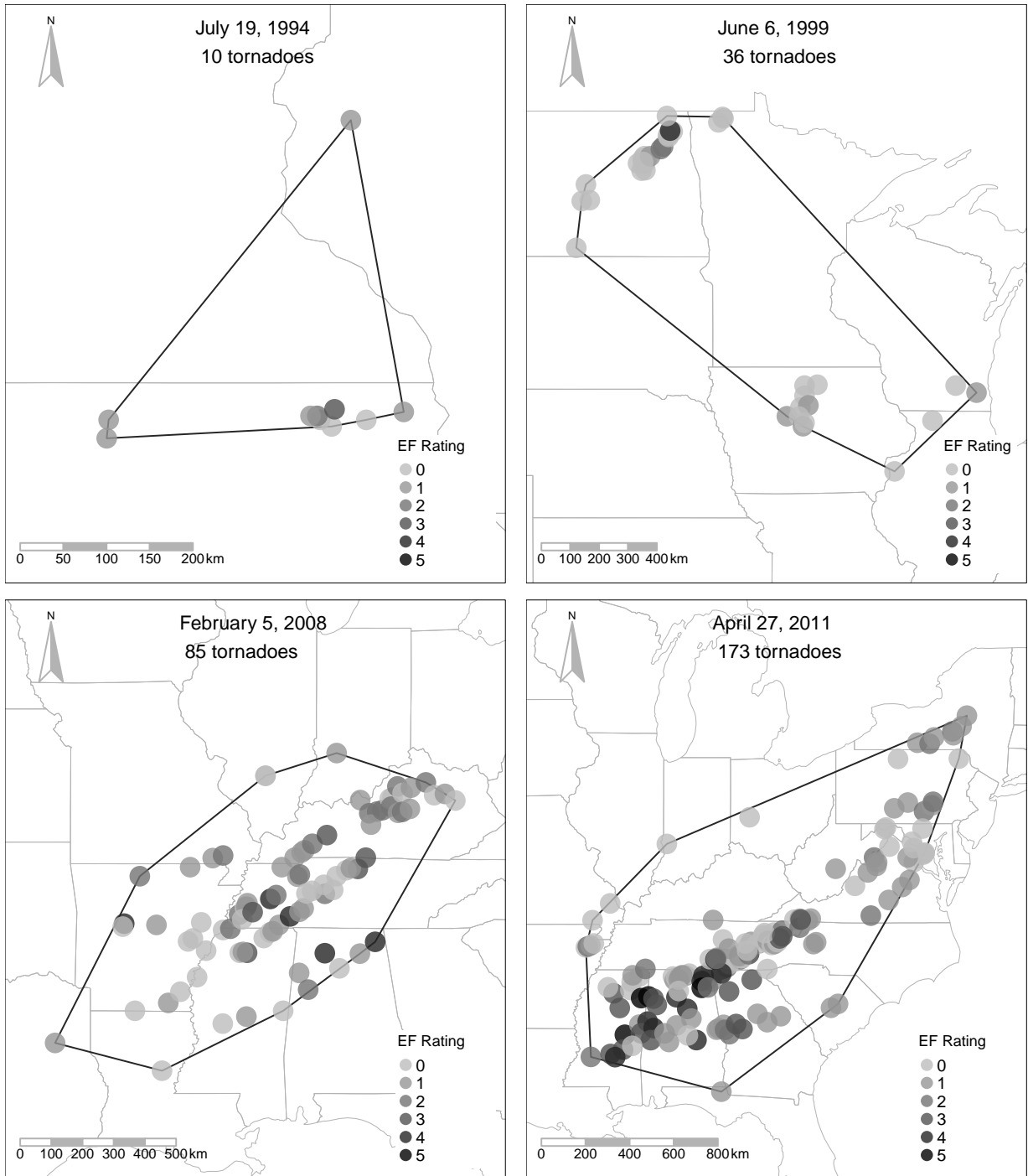
613 **Fig. 8.** Estimated probability of at least 30 tornadoes given an outbreak of at least ten tornadoes  
 614 and the regression model. The predicted count from the model is a parameter in a negative  
 615 binomial distribution with cluster area set at 400,000 km<sup>2</sup> and shallow-level bulk shear is set  
 616 to its mean value. . . . . 43

617 **Fig. 9.** Estimated probability of at least 30 tornadoes given an outbreak of at least ten tornadoes and  
 618 the regression model across a range of CAPE and deep-layer bulk shear values holding the  
 619 shallow-layer bulk shear at a mean value. . . . . 44

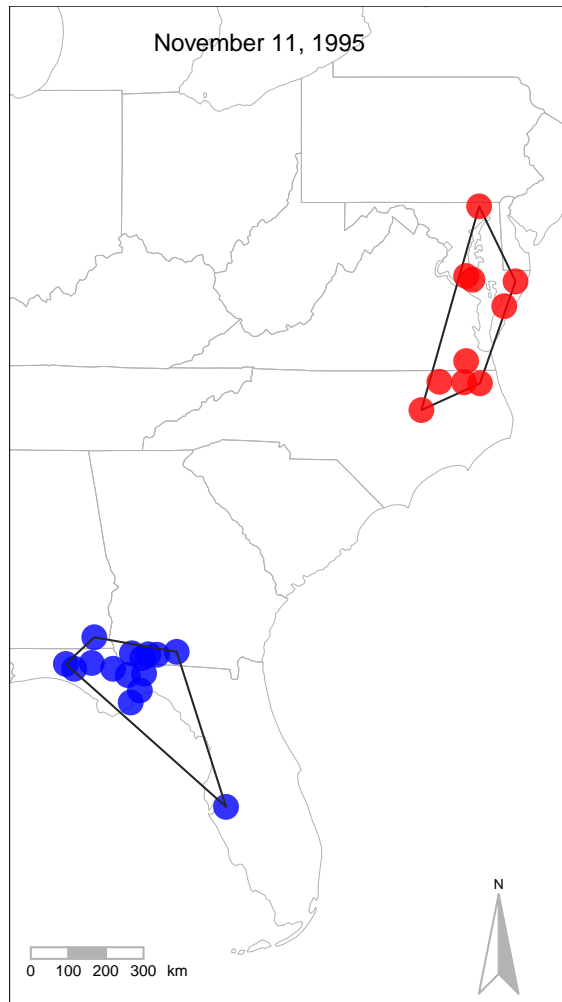
620 **Fig. 10.** Observed cluster-level casualty counts versus predicted rates from a negative binomial re-  
 621 gression. Clusters without casualties are plotted at the far left. The thin black line is the line  
 622 of best fit. The thick line is the slope of the model indicating the relationship between the  
 623 observed and predicted tornado counts and the associated standard error. . . . . 45

624 **Fig. 11.** Probability of at least 50 tornado casualties as a function of deep-layer bulk shear (left panel)  
 625 and CAPE (right panel) and modulated by the number of people in harm’s way. The other  
 626 variables are set at their mean values and year is set at 2018. . . . . 46

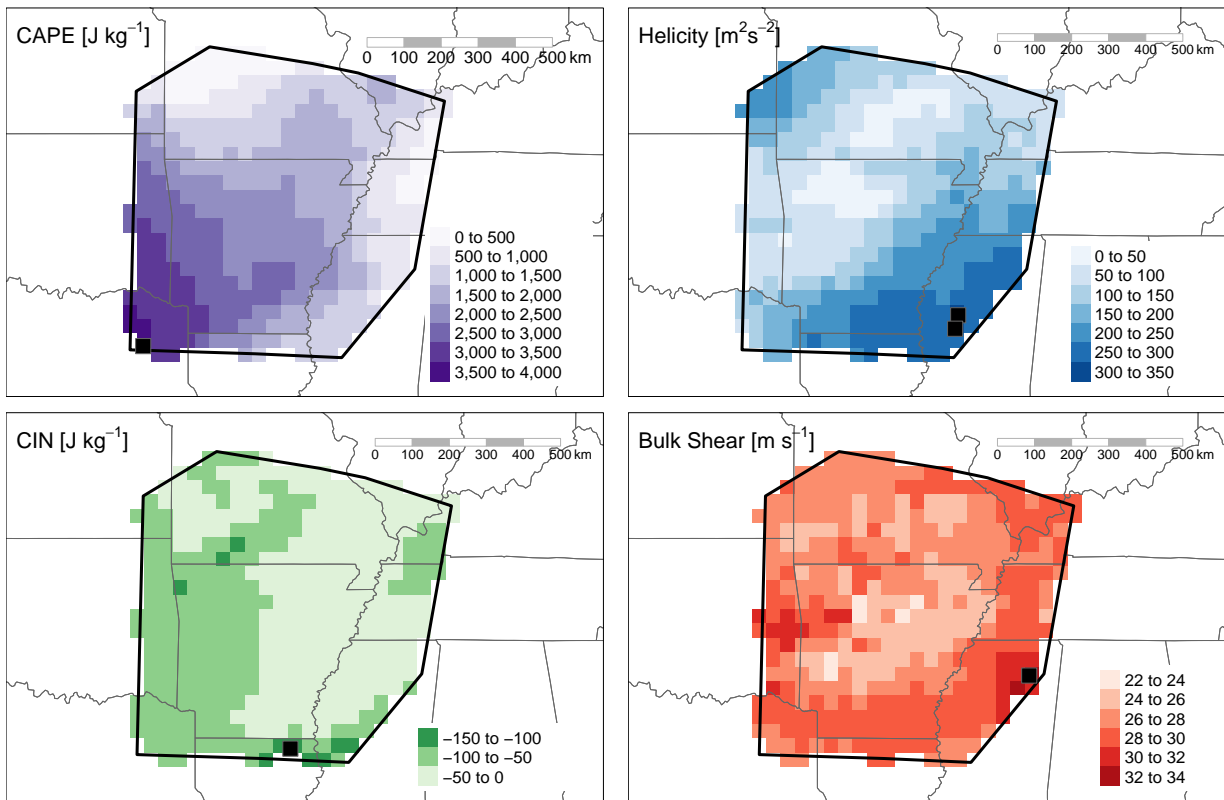
627 **Fig. 12.** Probability of at least 25 tornado casualties as a function of deep-layer bulk shear and CAPE  
628 and modulated by location for two *hypothetical* outbreaks, one centered over Sioux City,  
629 Iowa, and the other centered over Birmingham, Alabama. The shallow-layer bulk shear is  
630 set to its mean value, year is set to 2018, and population is set to 4M. . . . . 47



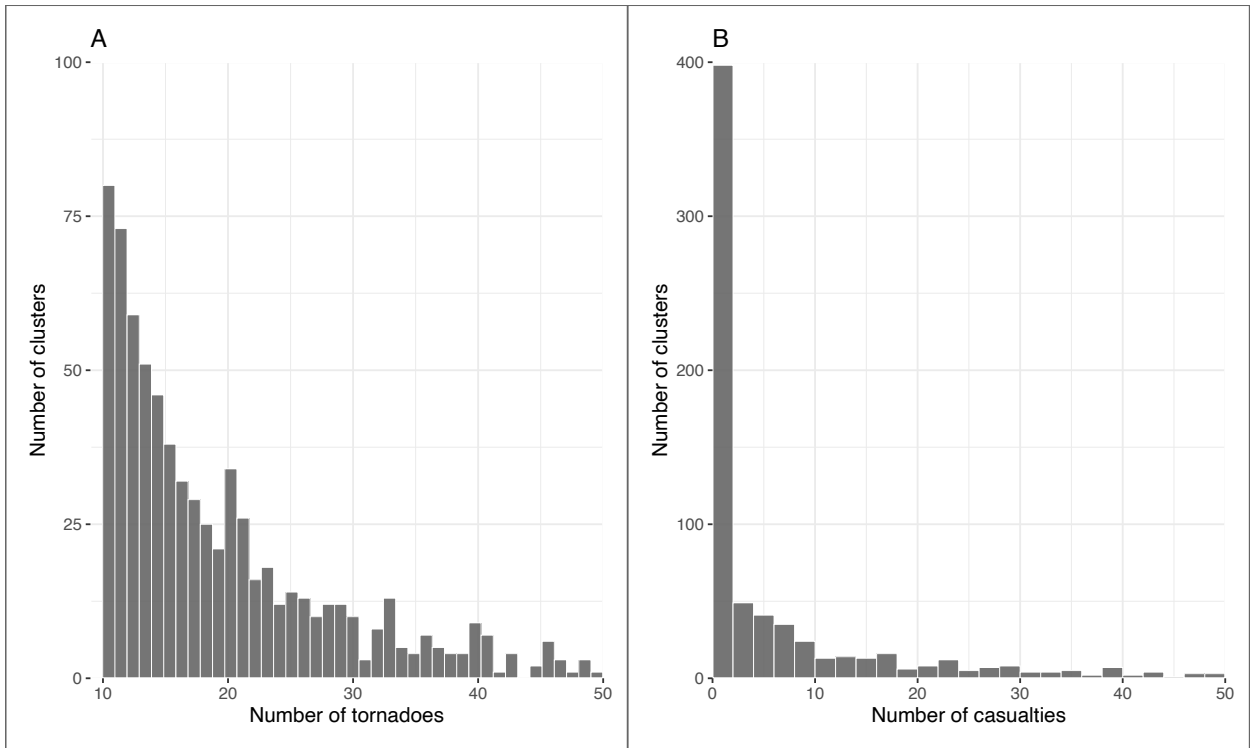
631 FIG. 1. Example tornado clusters. Each point is the tornadogenesis location shaded by EF rating. The black  
 632 line is the spatial extent of the tornadoes occurring on that convective day and is defined by the minimum convex  
 633 hull encompassing the set of locations.



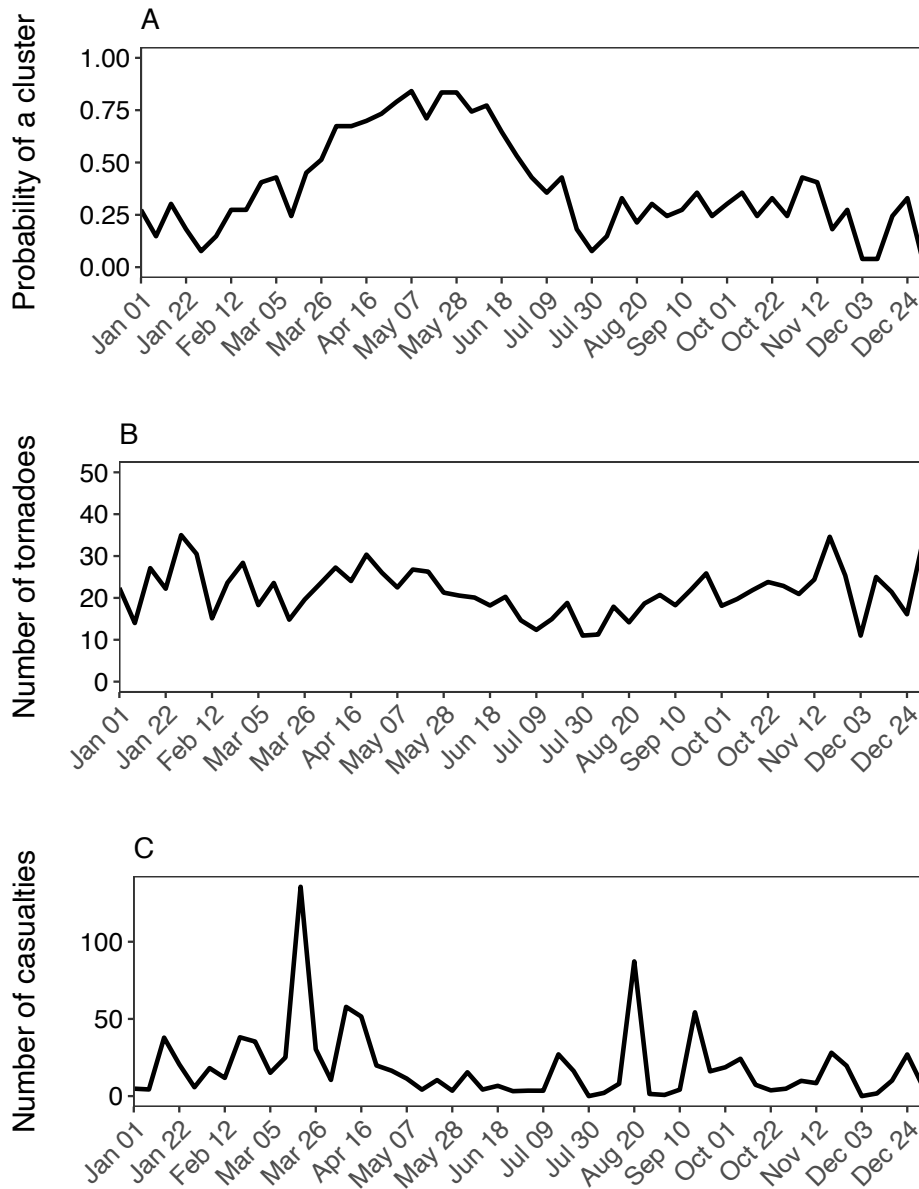
634 FIG. 2. Example of multiple clusters on a single convective day. Each point is a tornado genesis location.  
635 The black line is the spatial extent of the tornadoes for each cluster and is defined by the minimum convex hull  
636 encompassing the set of locations



637 FIG. 3. Example of the environmental factors for the May 6, 2003. The black line is the spatial extent of the  
 638 cluster on that convective day. Shading represents the intensity of the environment. CAPE is purple, helicity is  
 639 blue, CIN is green, and deep layer shear is red. The black square is the location of the maximum value for the  
 640 environmental factor.

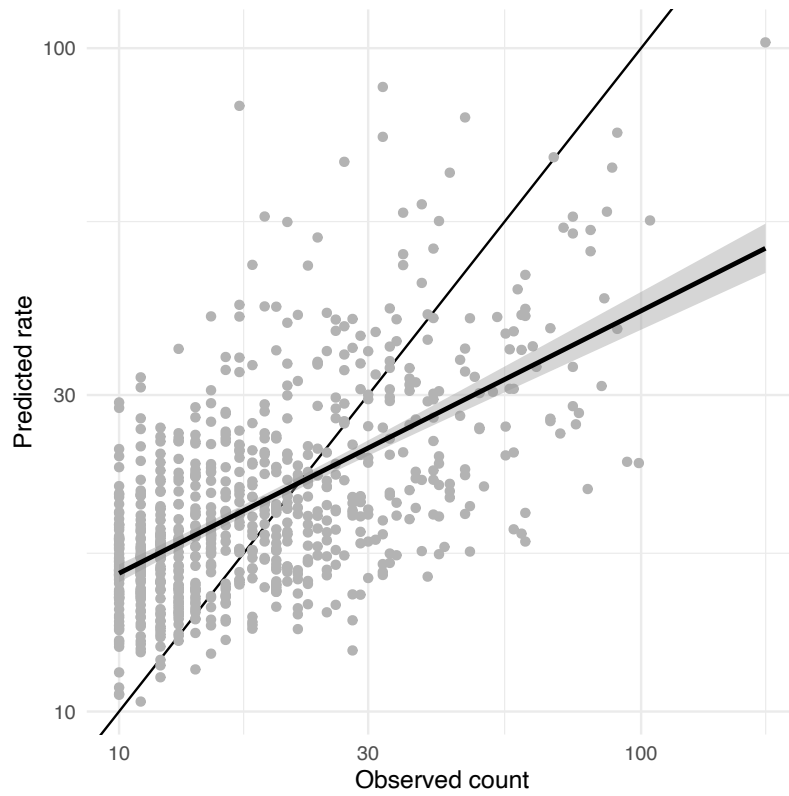


641 FIG. 4. Histograms of the number of clusters by number of tornadoes (A) and number of clusters by number of  
 642 casualties (B). The histograms are right-truncated at 50 to show detail on the left side of the distributions. Only  
 643 clusters with at least ten tornadoes are considered in this study.

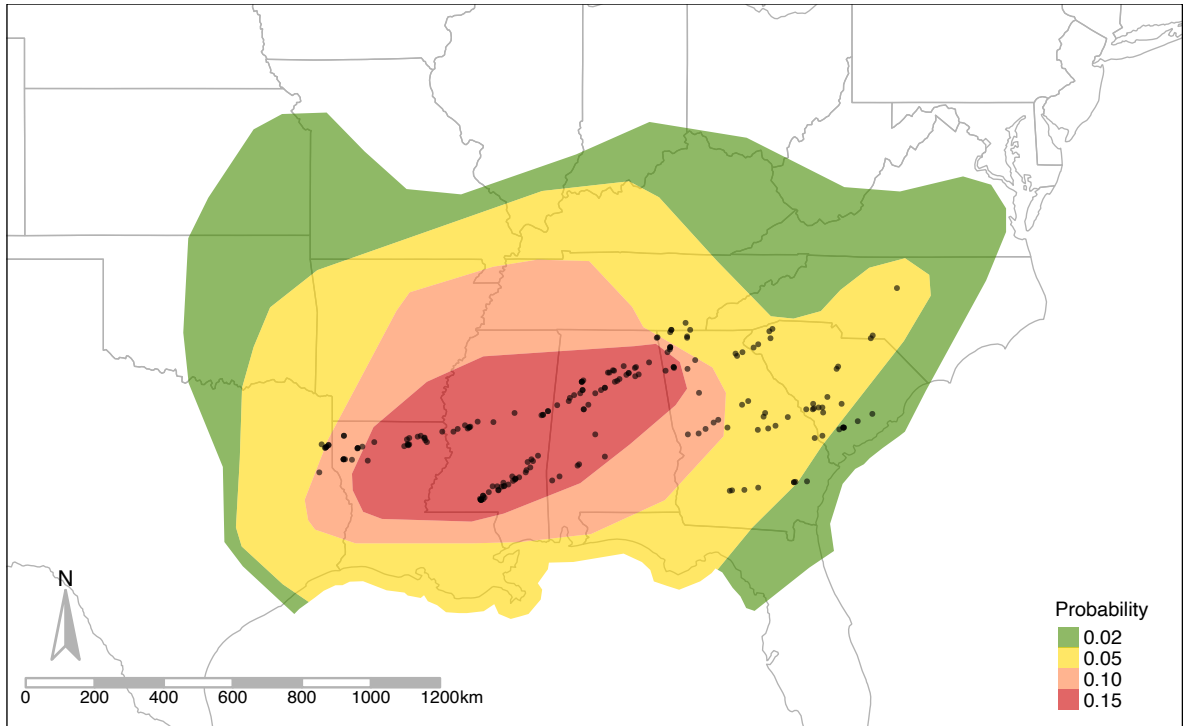


644 FIG. 5. Probability of a cluster (A), average number of tornadoes per cluster (B), and average number of  
 645 casualties per 1 000 000 people per cluster (C) by week of the year.

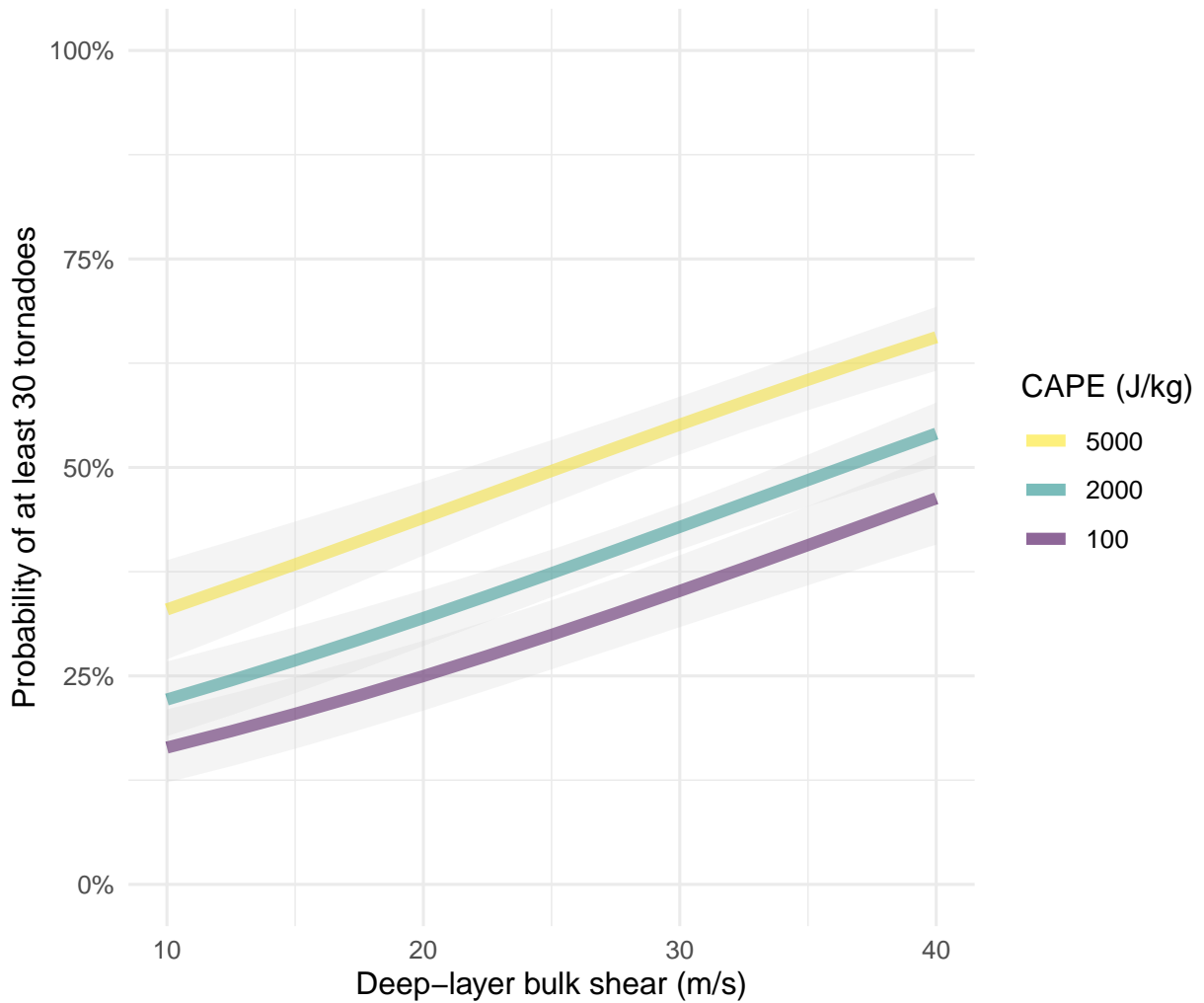




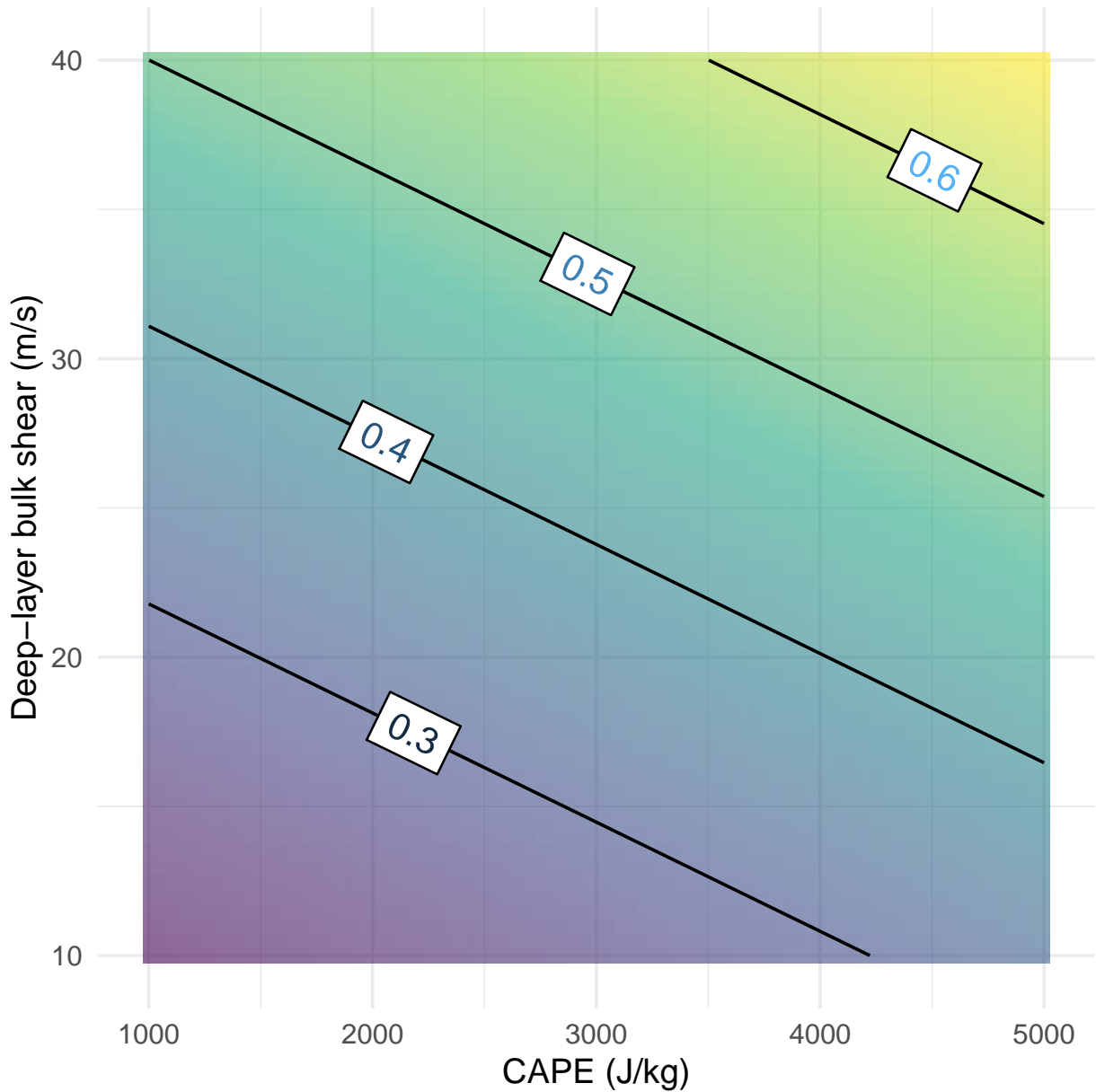
646 FIG. 6. Observed cluster-level tornado counts versus predicted rates from a negative binomial regression. The  
647 thin black line is the line of best fit. The thick line is the slope of the model indicating the relationship between  
648 the observed and predicted tornado counts and the associated standard error.



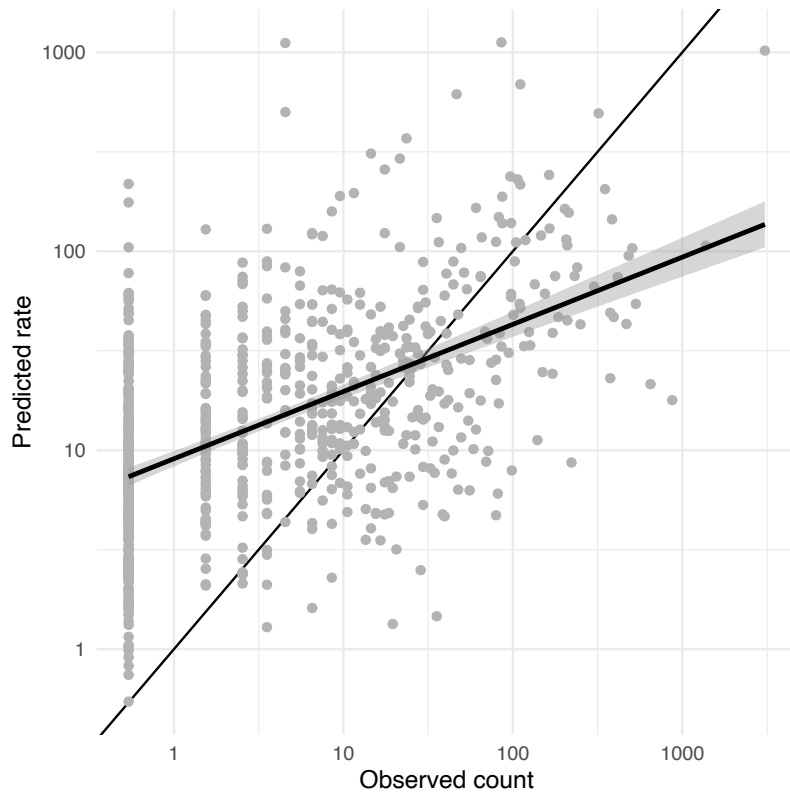
649 FIG. 7. Convective outlook issued by the Storm Prediction Center at 12 UTC on April 12, 2020 and the  
 650 locations of tornado reports over the 24-hr period starting at that time. The outlook category numbers indicate  
 651 the chance of observing severe weather within 40 km of any location. The convective outlook shapefiles are from  
 652 [www.spc.noaa.gov/cgi-bin/spc/getacrange.pl?date0=20200412&date1=20200412](http://www.spc.noaa.gov/cgi-bin/spc/getacrange.pl?date0=20200412&date1=20200412) and the tornado  
 653 reports are from [www.spc.noaa.gov/climo/reports/200412\\_rpts.html](http://www.spc.noaa.gov/climo/reports/200412_rpts.html).



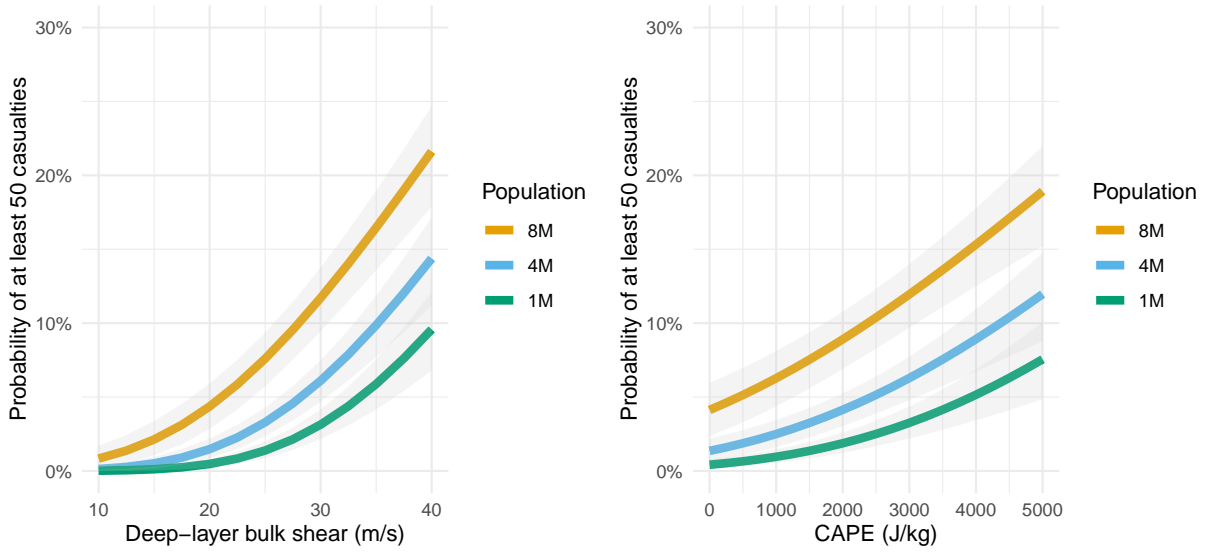
654 FIG. 8. Estimated probability of at least 30 tornadoes given an outbreak of at least ten tornadoes and the  
 655 regression model. The predicted count from the model is a parameter in a negative binomial distribution with  
 656 cluster area set at 400,000 km<sup>2</sup> and shallow-level bulk shear is set to its mean value.



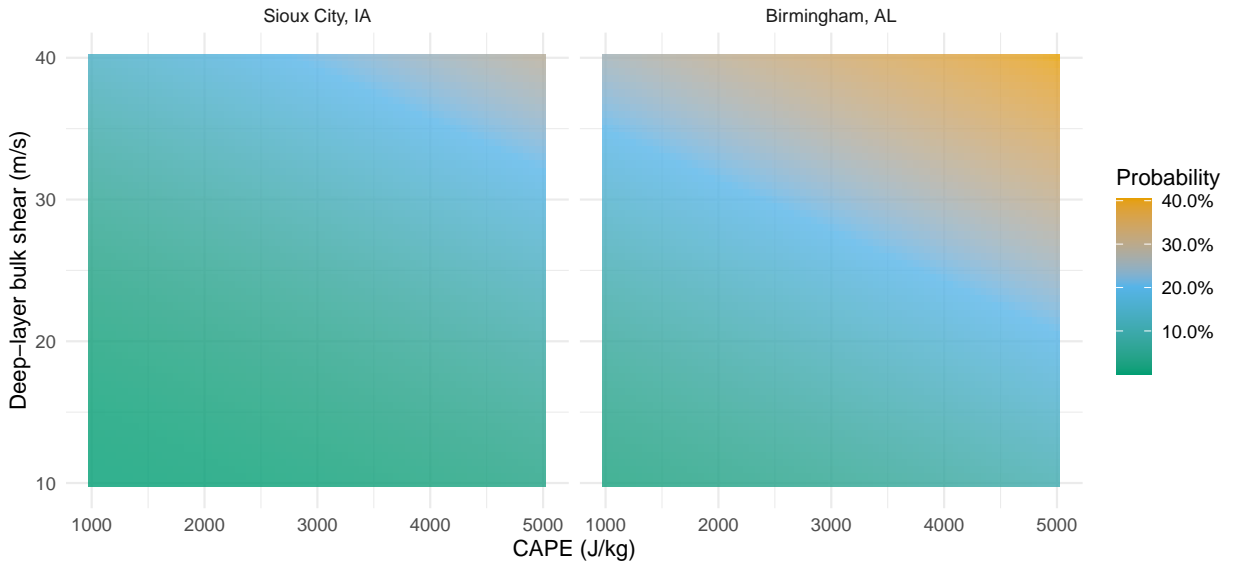
657 FIG. 9. Estimated probability of at least 30 tornadoes given an outbreak of at least ten tornadoes and the  
 658 regression model across a range of CAPE and deep-layer bulk shear values holding the shallow-layer bulk shear  
 659 at a mean value.



660 FIG. 10. Observed cluster-level casualty counts versus predicted rates from a negative binomial regression.  
661 Clusters without casualties are plotted at the far left. The thin black line is the line of best fit. The thick line  
662 is the slope of the model indicating the relationship between the observed and predicted tornado counts and the  
663 associated standard error.



664 FIG. 11. Probability of at least 50 tornado casualties as a function of deep-layer bulk shear (left panel) and  
 665 CAPE (right panel) and modulated by the number of people in harm's way. The other variables are set at their  
 666 mean values and year is set at 2018.



667 FIG. 12. Probability of at least 25 tornado casualties as a function of deep-layer bulk shear and CAPE and  
 668 modulated by location for two *hypothetical* outbreaks, one centered over Sioux City, Iowa, and the other centered  
 669 over Birmingham, Alabama. The shallow-layer bulk shear is set to its mean value, year is set to 2018, and  
 670 population is set to 4M.